SUPPLEMENTARY

Figures

Figure S1. ^{1}H NMR spectrum of 4,4‘-di-*tert*-butyl-2,2‘-bipyridin-*N*-oxide (300 MHz, $CDCl_3$, 298 K).

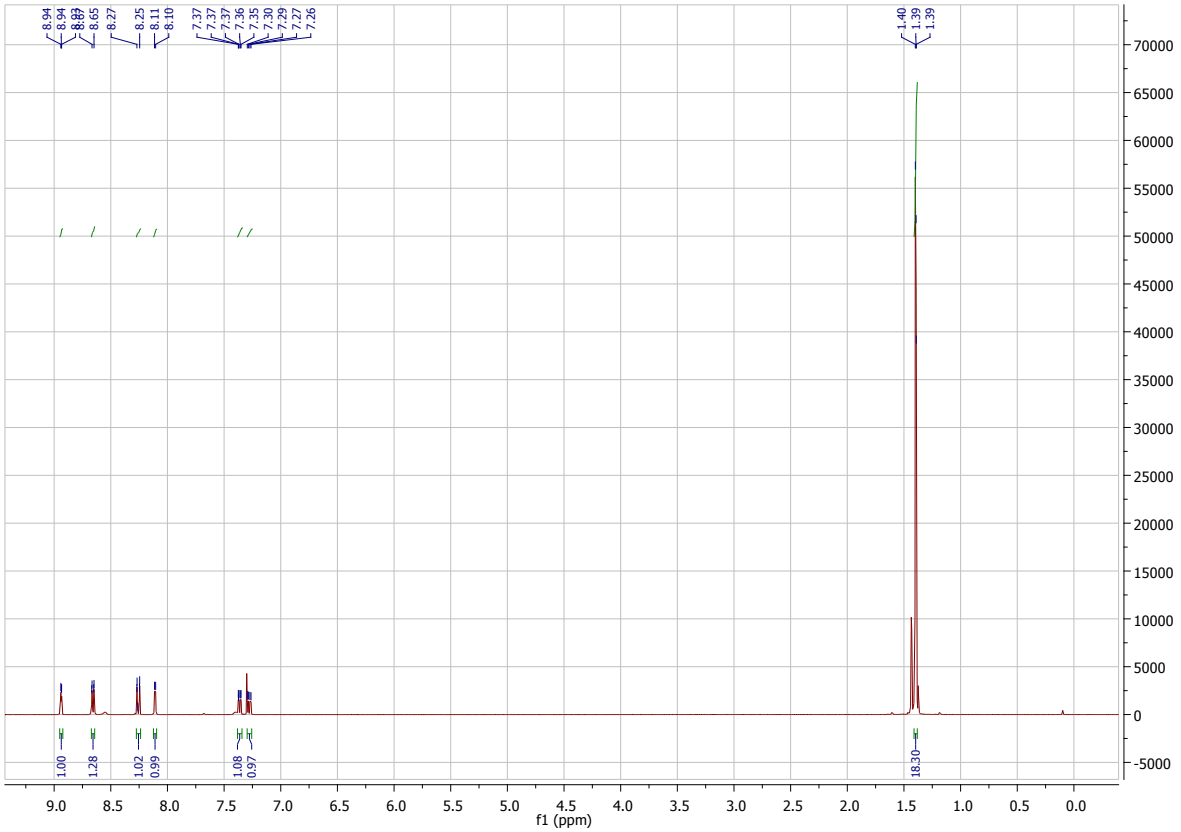

Figure S2. $^{13}C\{^{1}H\}^{72}$ NMR spectrum of 4,4‘-di-*tert*-butyl-2,2‘-bipyridin-*N*-oxide (300 MHz, $CDCl_3$, 298 K).

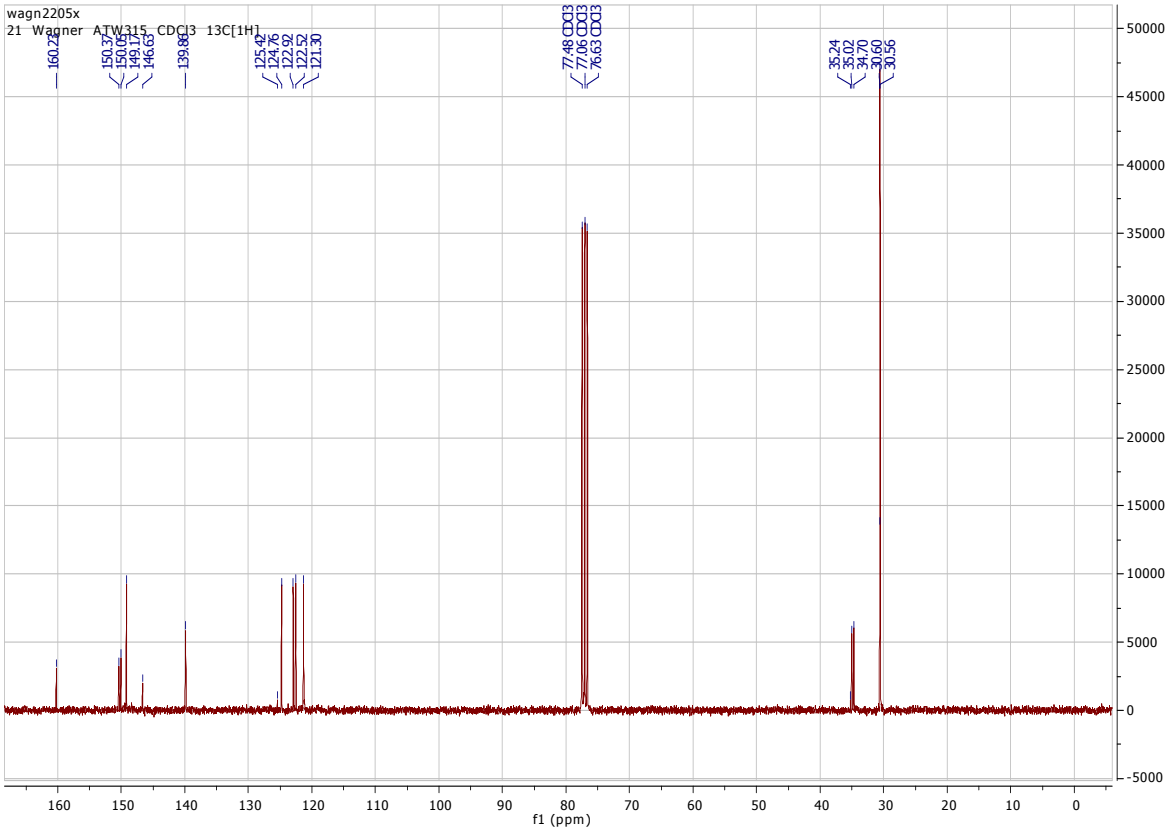

Figure S3. ^{1}H NMR spectrum of 4,4‘-Di-*tert*-butyl-6-(tetrazol-5-yl)-2,2‘-bipyridin ($HN_4{}^{t}$bubipy·HCl) (300 MHz, $CDCl_3$, 298 K).

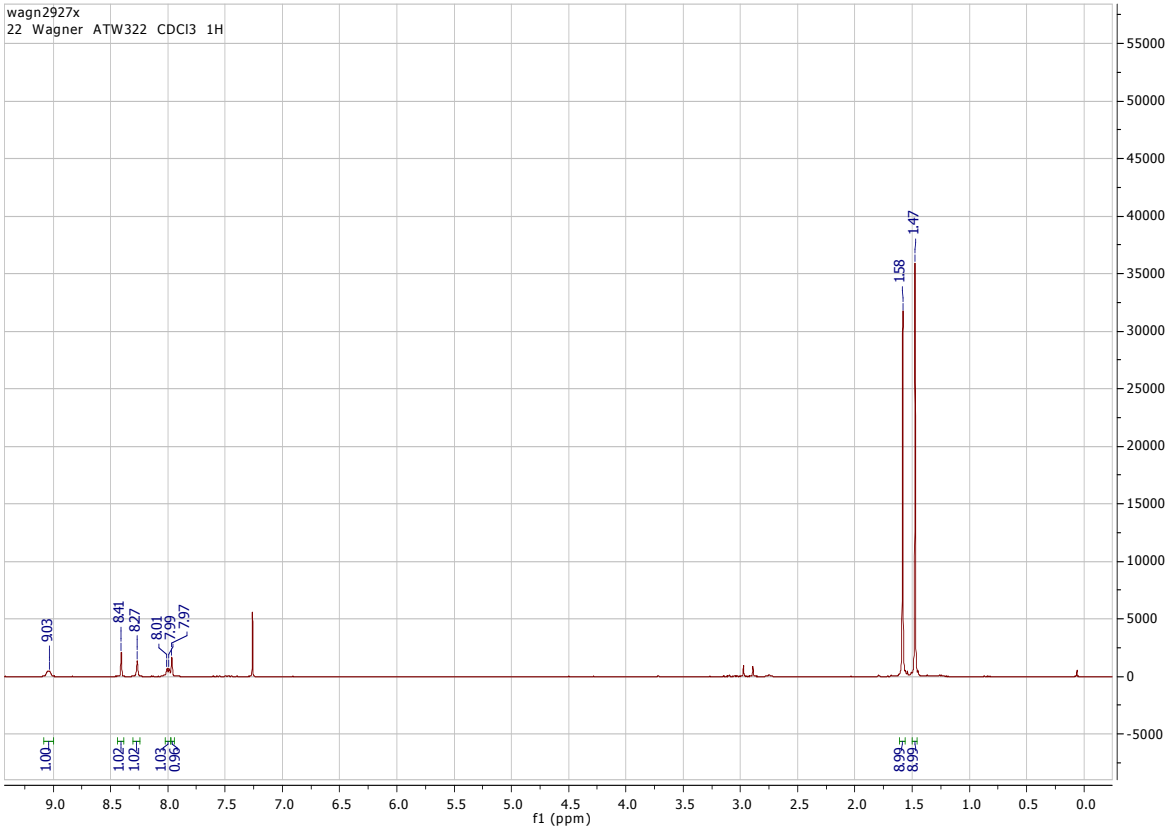

Figure S4. $^{13}C\{^{1}H\}$ NMR spectrum of 4,4‘-Di-*tert*-butyl-6-(tetrazol-5-yl)-2,2‘-bipyridin ($HN_4{}^{t}$bubipy·HCl) (300 MHz, $CDCl_3$, 298 K).

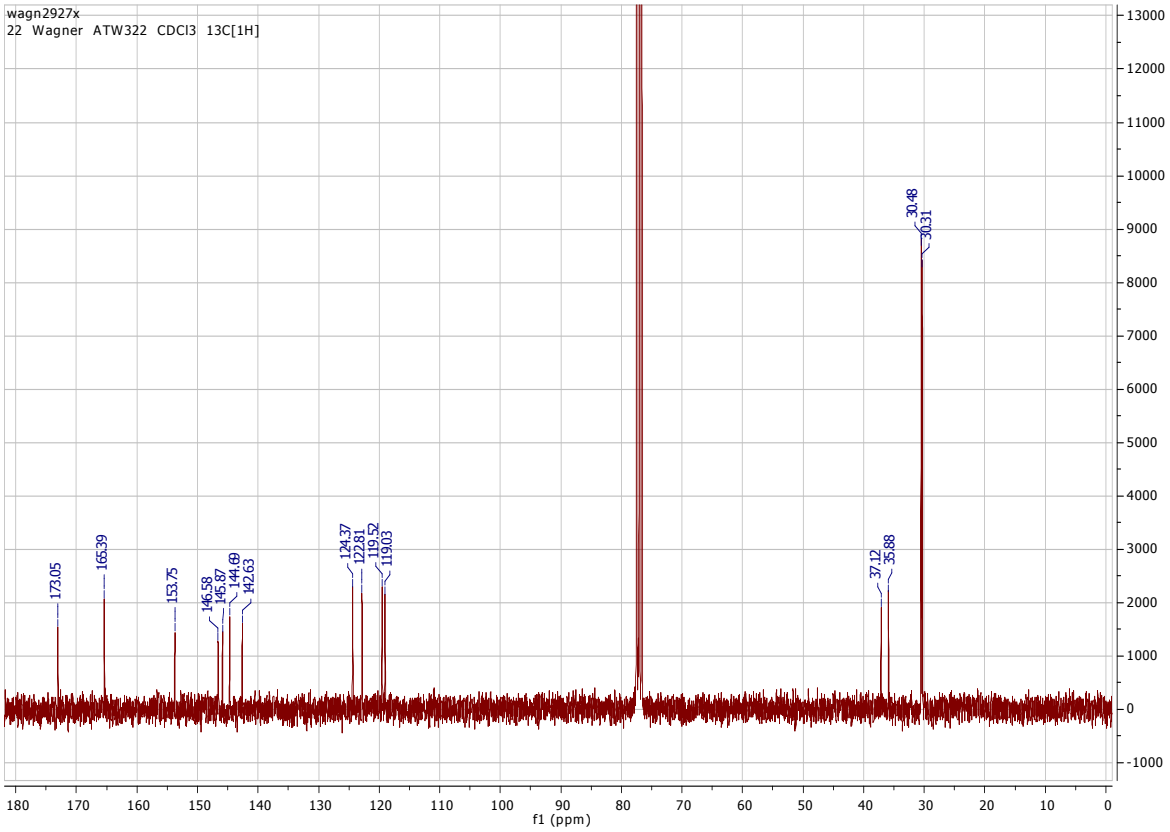

Figure S5. ^{1}H NMR spectrum of $HN_4{}^{t}$bubipy·HNO_3 (300 MHz, $CDCl_3$, 298 K).

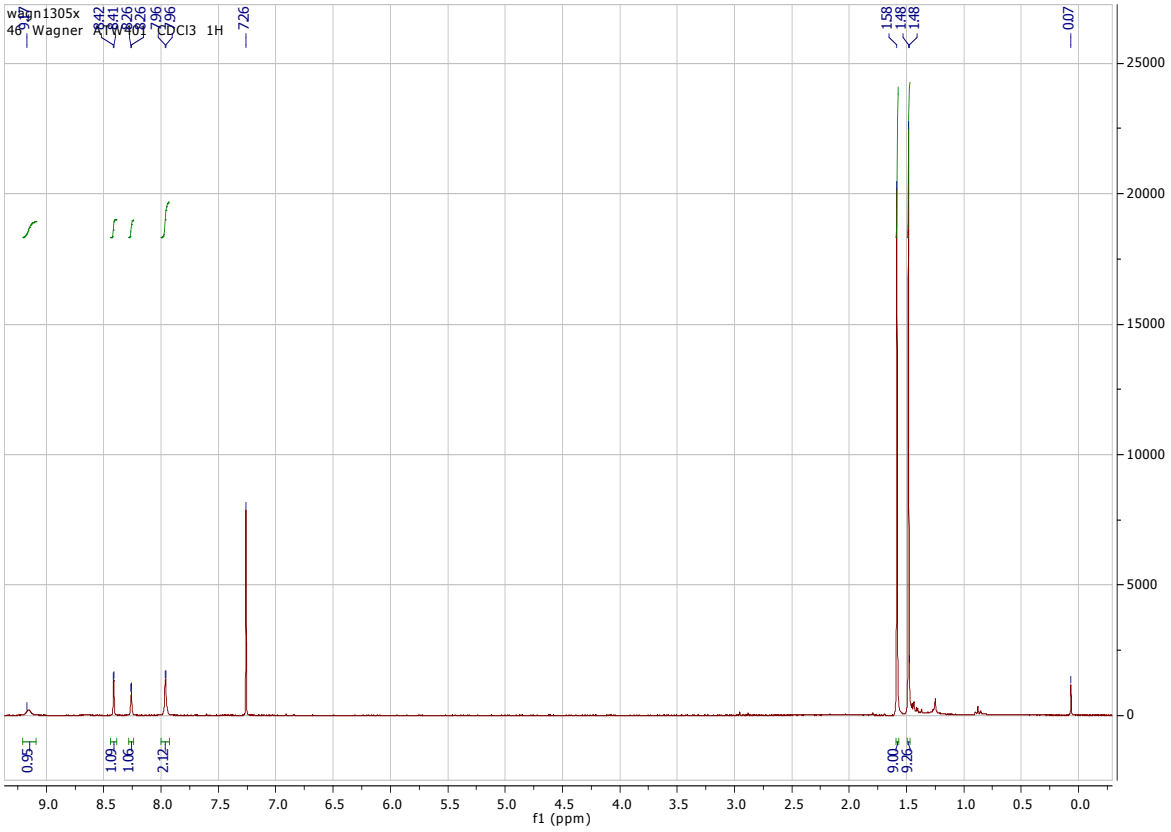

Figure S6. $^{13}C\{^{1}H\}$ NMR spectrum of HN_4[t]bubipy·HNO_3 (300 MHz, $CDCl_3$, 298 K).

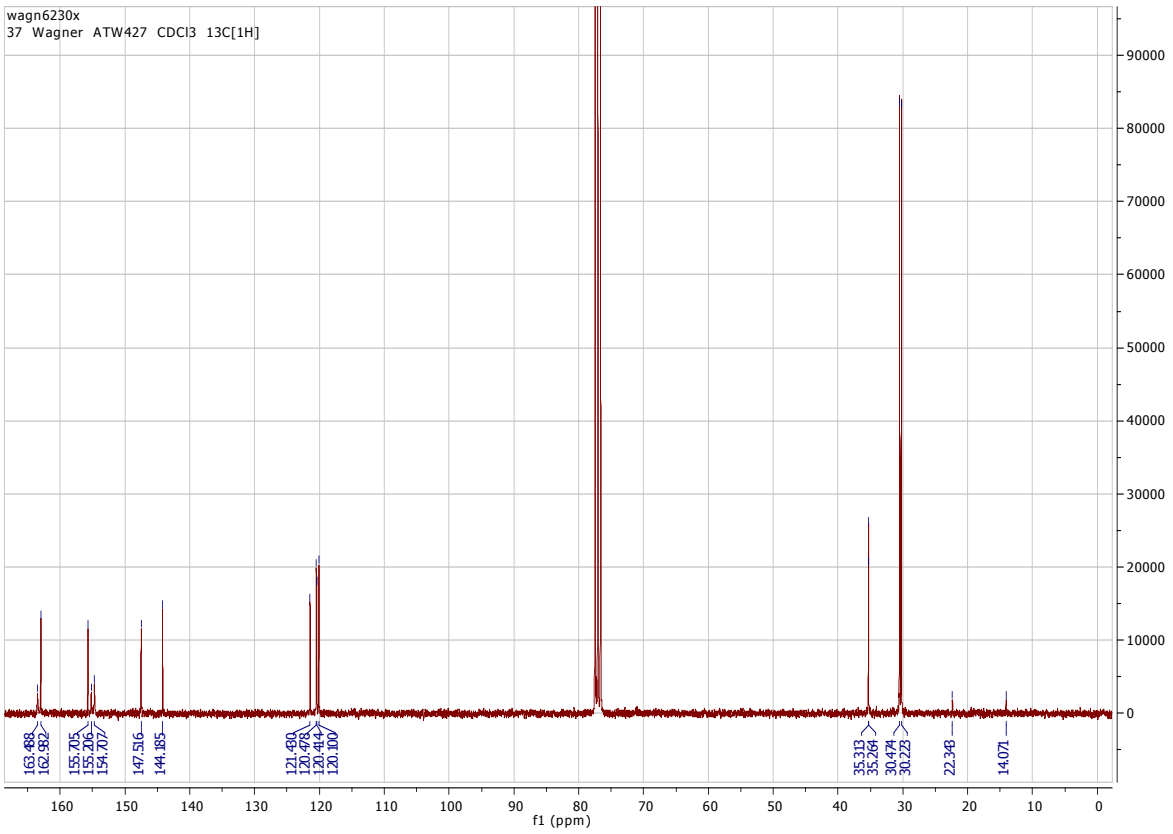

ESI MS Spectra of $[H_2N_4{}^tbubipy]^+[Sm(N_4{}^tbubipy)(NO_3)_3(H_2O)]^-$ and $[H_2N_4{}^tbubipy]^+[Eu(N_4{}^tbubipy)(NO_3)_3(H_2O)]^-$.

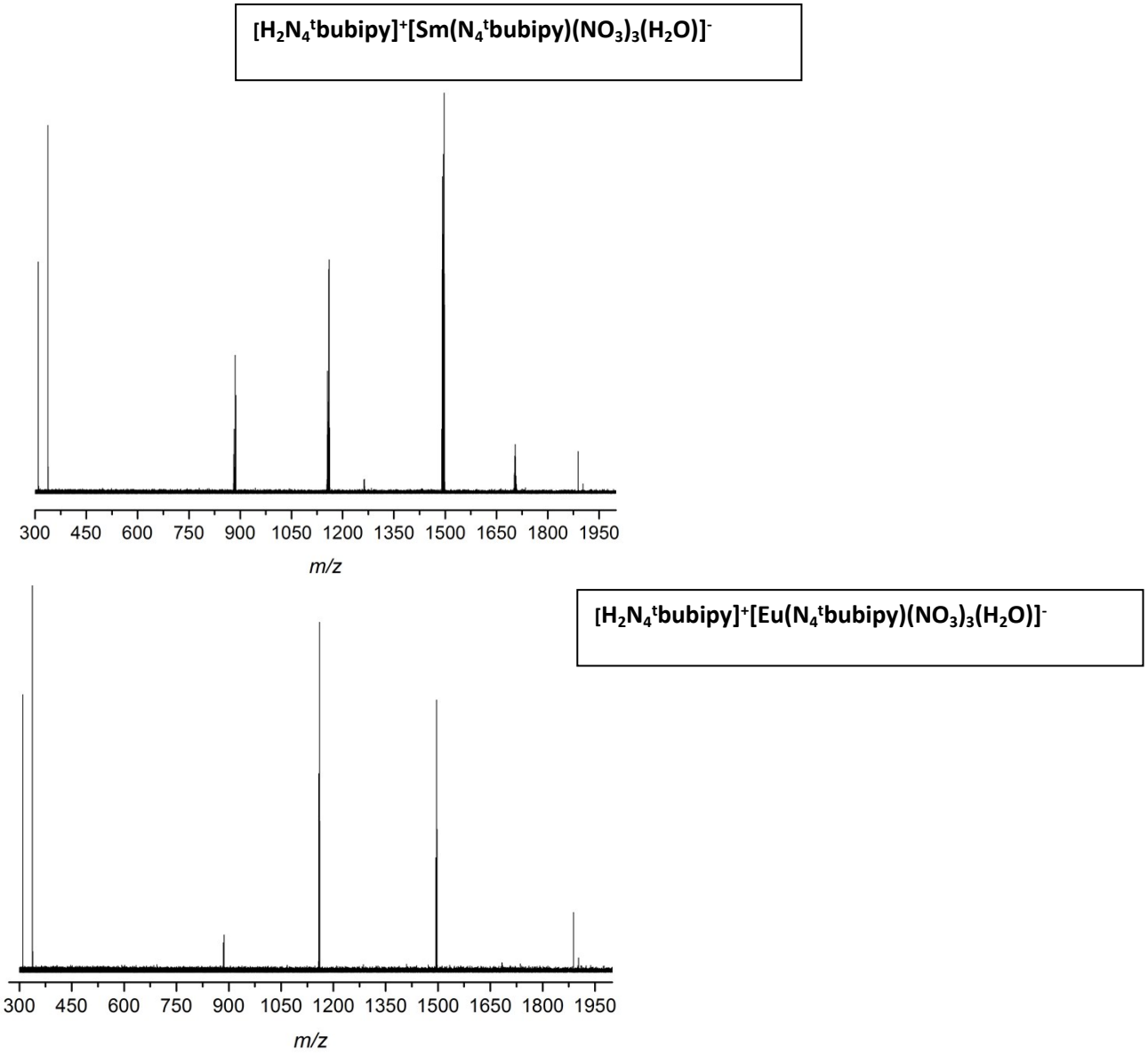

Figure S7: ESI-MS spectrum of single crystals of dissolved acetonitrile. Top: Complete positive ion spectrum of $[H_2N_4{}^tbubipy]^+[Sm(N_4{}^tbubipy)(NO_3)_3(H_2O)]^-$. Bottom: Complete positive ion spectrum of $[H_2N_4{}^tbubipy]^+[Eu(N_4{}^tbubipy)(NO_3)_3(H_2O)]^-$ (m/z = 337 = $[H_2N_4{}^tbubipy]^+$; m/z = 309 = $[H_2N_4{}^tbubipy\text{-}N_2]^+$; m/z = 1158.55 amu $[H_2N_4{}^tbubipy]^+[Sm(N_4{}^tbubipy)(NO_3)_3]^-$ (top) m/z = 1159.68 amu = $[H_2N_4{}^tbubipy]^+[Eu(N_4{}^tbubipy)(NO_3)_3]^-$ (bottom); m/z = 1496.80 = $[Sm(N_4{}^tbubipy)_3(HN_4{}^tbubipy)+H]^+$ (top); m/z = 1495.98 = $[Eu(N_4{}^tbubipy)_3(HN_4{}^tbubipy)+H]^+$ (bottom)).

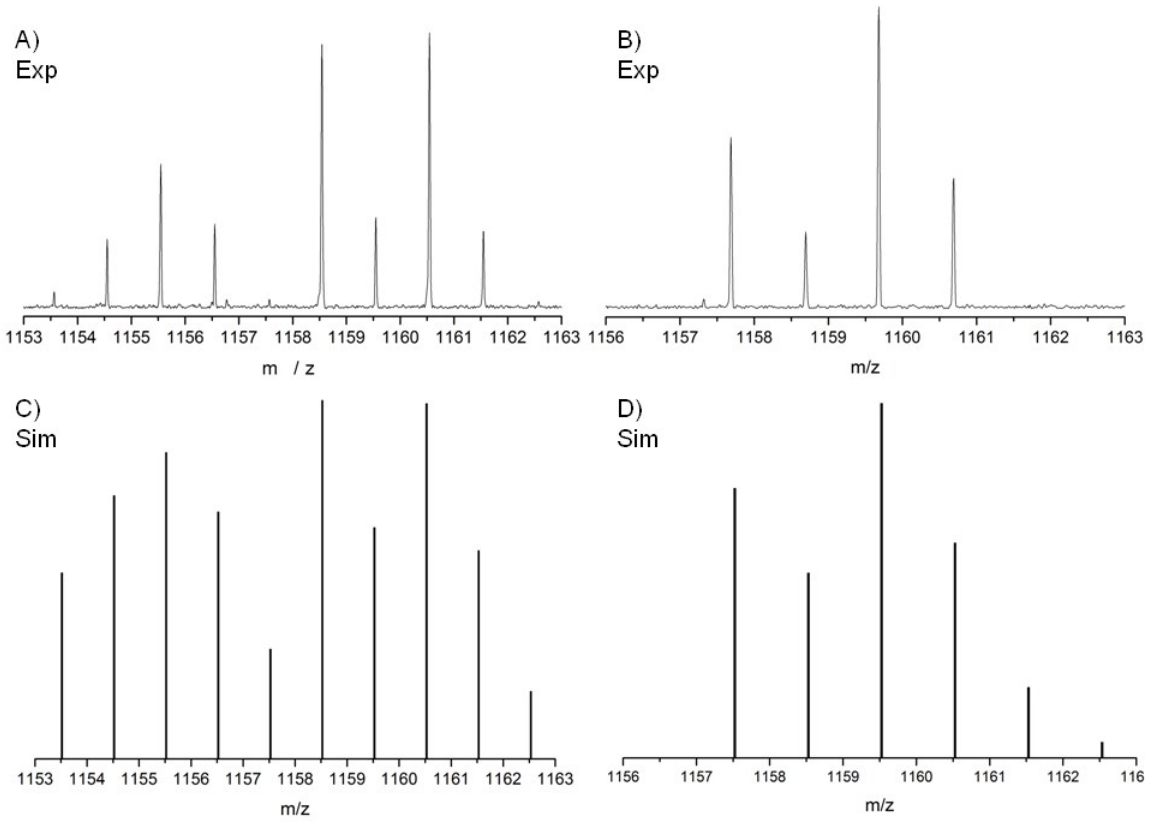

Figure S8: A) Measured spectrum of $[H_2N_4{}^tbubipy]^+[Sm(N_4{}^tbubipy)(NO_3)_3(H_2O)]^-$. B) Measured spectrum of $[H_2N_4{}^tbubipy]^+[Eu(N_4{}^tbubipy)(NO_3)_3(H_2O)]^-$. C) Simulated spectrum of $[Sm(N_4{}^tbubipy)_3+H]^+$. D) Simulated spectrum of $[Eu(N_4{}^tbubipy)_3+H]^+$.

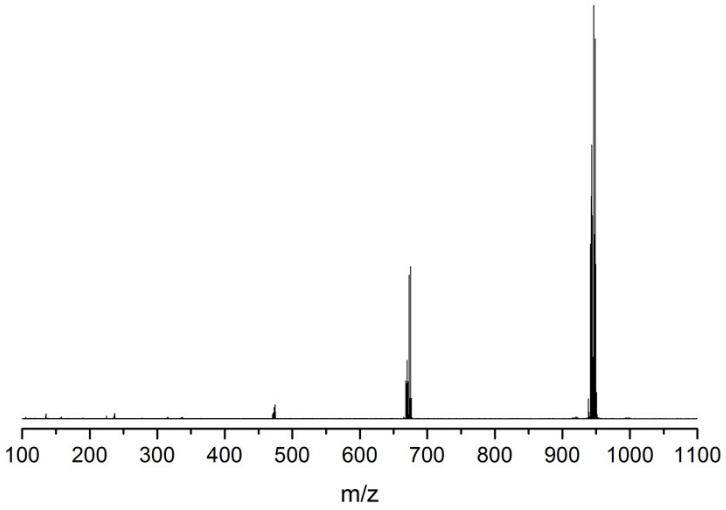

Figure S9: Complete negative ion spectrum of $[H_2N_4{}^tbubipy]^+[Sm(N_4{}^tbubipy)(NO_3)_3(H_2O)]^-$ (m/z = 673.10 = $[Sm(N_4{}^tbubipy)(NO_3)_3]^-$; m/z = 946.31 = $[Sm(N_4{}^tbubipy)_2(NO_3)_2]^-$)

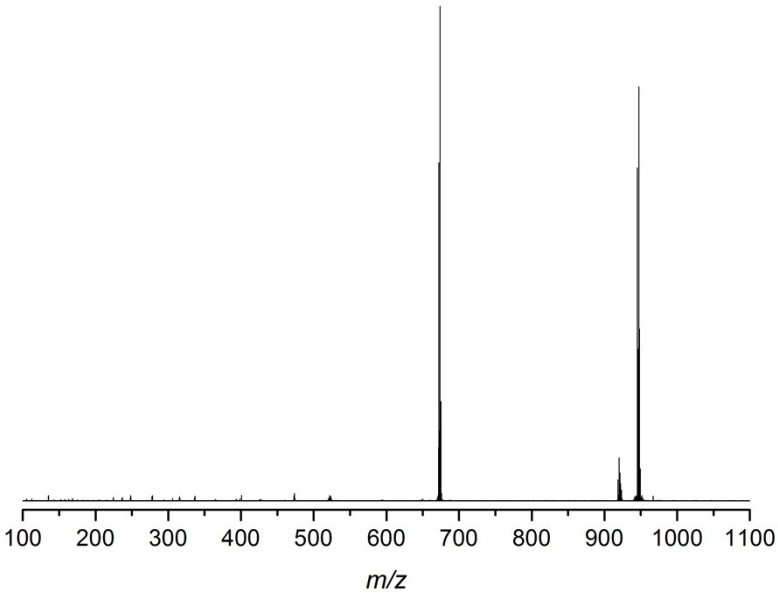

Figure S10: Complete negative ion spectrum of $[H_2N_4{}^tbubipy]^+[Sm(N_4{}^tbubipy)(NO_3)_3]^-$ (m/z = 674.12 = $[Eu(N_4{}^tbubipy)(NO_3)_3]^-$; m/z = 947.34 =$[Eu(N_4{}^tbubipy)_2(NO_3)_2]^-$)

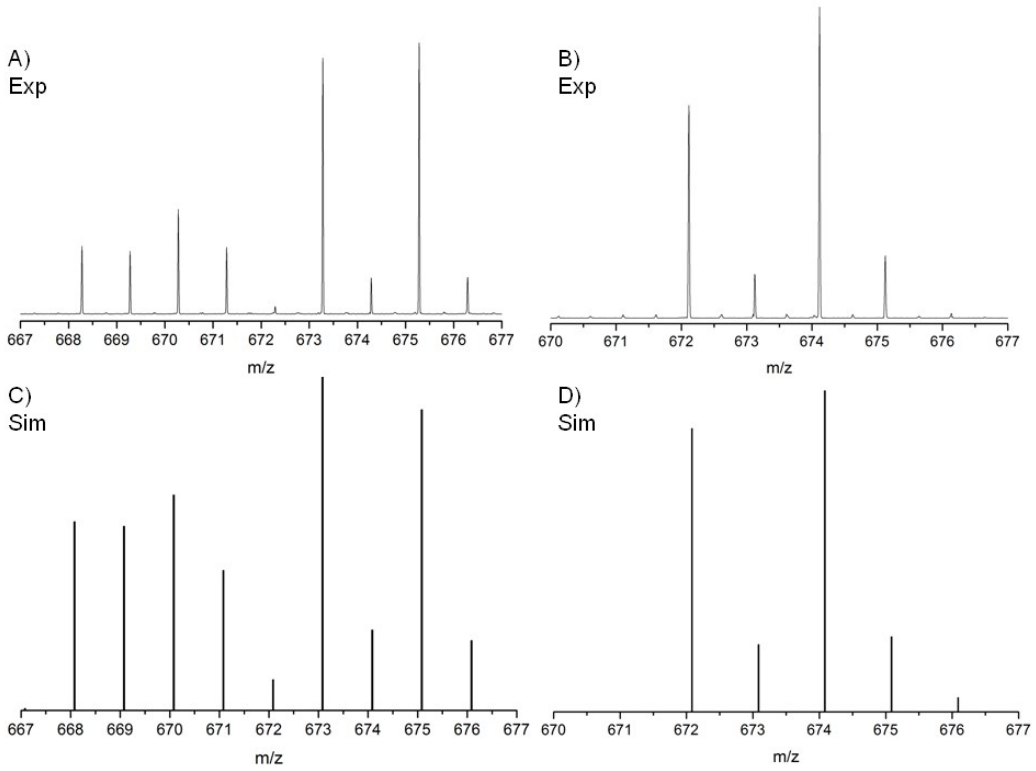

Figure S11: A) Measured spectrum of $[H_2N_4{}^tbubipy]^+[Sm(N_4{}^tbubipy)(NO_3)_3]^-$. B) Measured spectrum of $[H_2N_4{}^tbubipy]^+[Eu(N_4{}^tbubipy)(NO_3)_3]^-$. C) Simulated spectrum of $[Sm(N_4{}^tbubipy)(NO_3)_3]^-$. D) Simulated spectrum of $[Eu(N_4{}^tbubipy)(NO_3)_3]^-$.

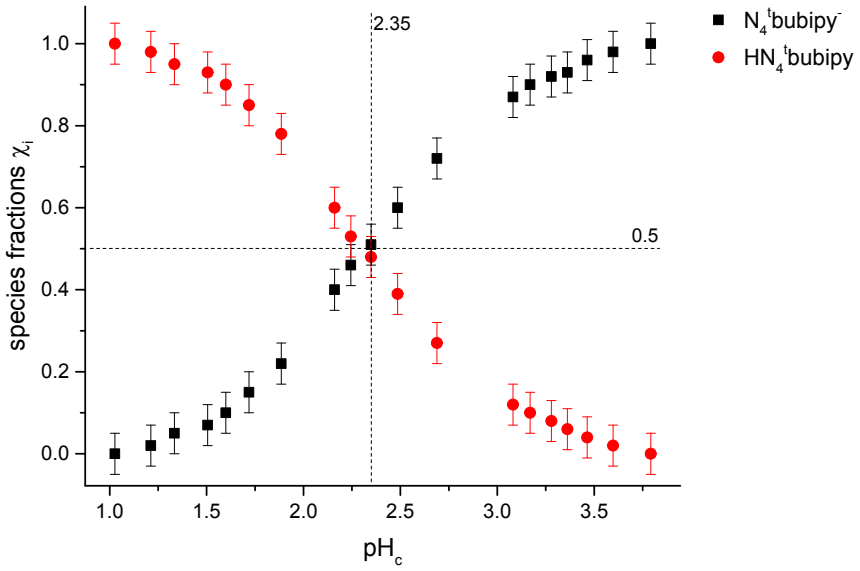

Figure S12: Species distribution of the protonated and deprotonated species of $HN_4^tbubipy$ with increasing pH_c in ethanol, 4.4 vol% H_2O.

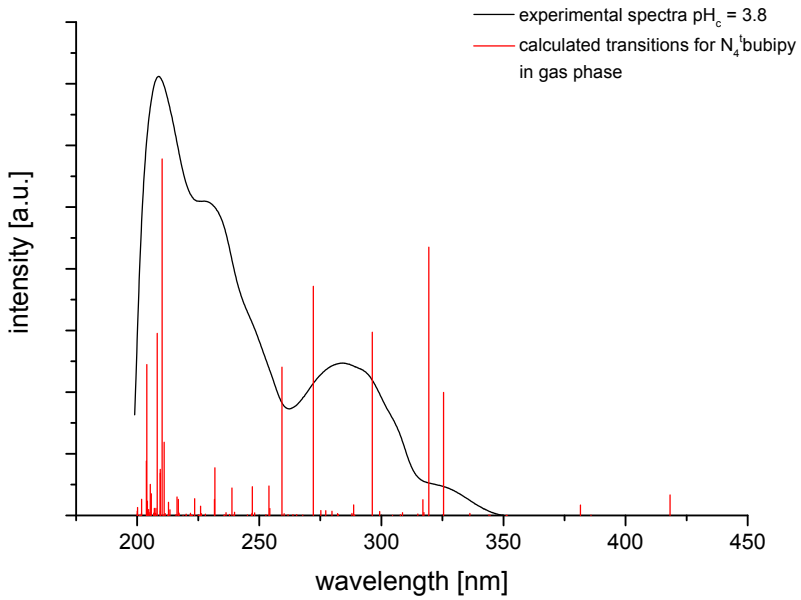

Figure S13: Experimental absorption spectra (black line) of $N_4^tbubipy^-$ and calculated excitation energies on B3-LYP/def-TZVP level accounting for a solvatochromic shift of 30 nm.

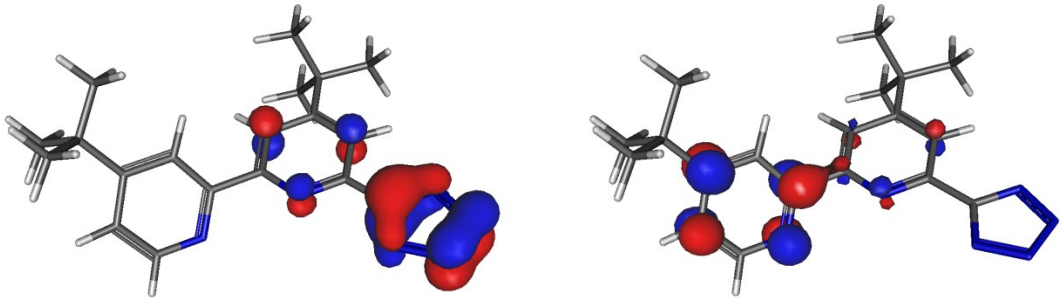

Figure S14: Calculated HOMO (left) and LUMO (right) orbitals of the deprotonated ligand $N_4{}^t$bubipy$^-$. Calculated on B3-LYP/def-TZVP level.

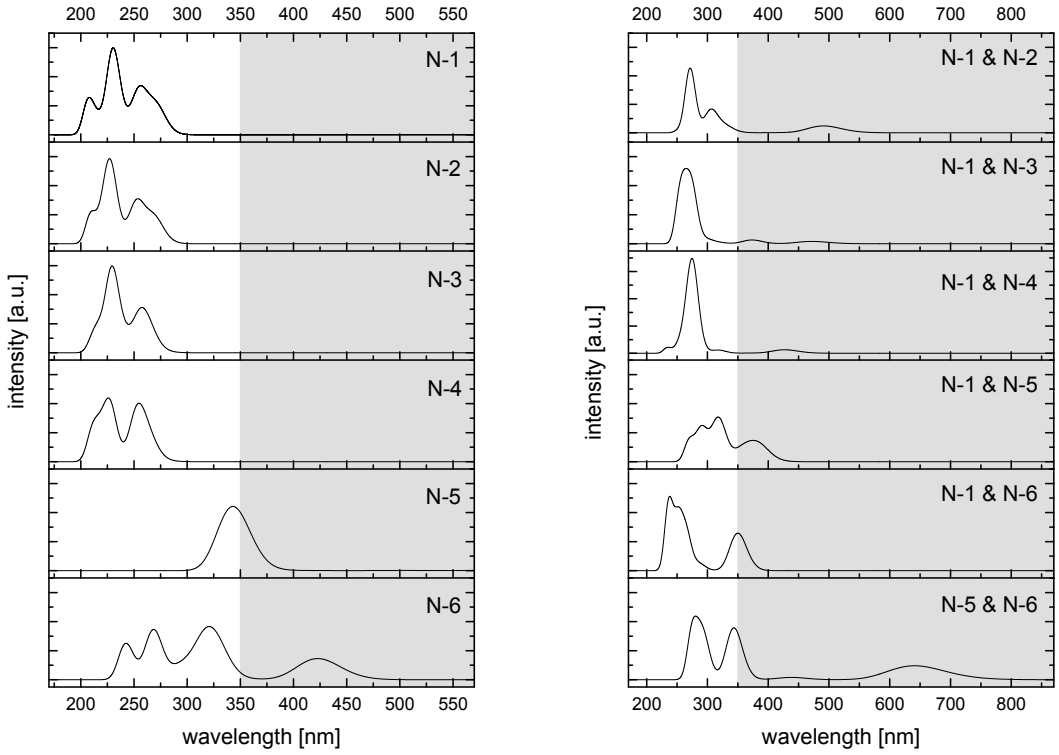

Figure S15: Computed absorption spectra of $HN_4{}^t$bubipy and $H_2N_4{}^t$bubipy$^+$ with protonation at various N atoms.. Solvatochromic shifts are not taken into account.

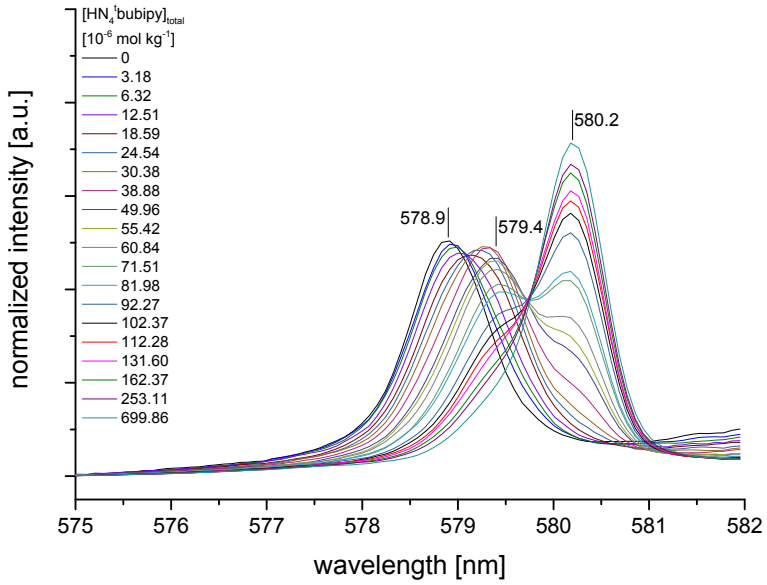

Figure S16: Normalized fluorescence spectra of the $^5D_0 \rightarrow {}^7F_0$ transition of Eu(III) as a function of the total ligand concentration in EtOH (4.4 vol.% H_2O). [Eu(III)] = $5 \cdot 10^{-5}$ mol/kg.

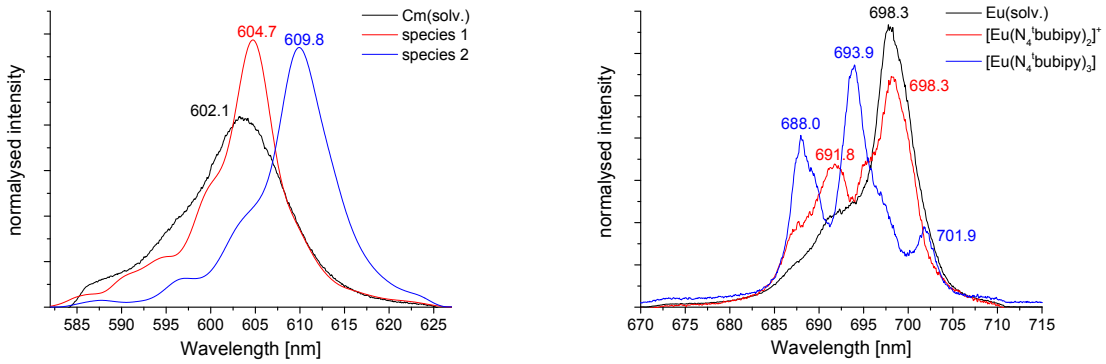

Figure S17: Single component spectra of the Cm(III) (left) and Eu(III) HN_4tbubipy (right) complexes.

Tables

Table S1: Calculated ground state energies of protonation at different positions of the HN_4[t]bubipy on DFT level and energy difference to the most stable structure.

protonation position	**E_h [H]**	**ΔE_h [H]**	**ΔE_h [kJ mol^{-1}]**
N-1	-1064.7947		
N-2	-1064.7888	0.0059	15.54
N-3	-1064.7862	0.0086	22.46
N-4	-1064.7778	0.0169	44.48
N-5	-1064.7321	0.0626	164.39
N-6	-1064.7782	0.0165	43.35

Table S2: Calculated interaction energies E_g in kJ mol^{-1} for [Cm(N_4[t]bubipy)$_3$] and [Gd(N_4[t]bubipy)$_3$] on MP2 level and difference in ground state energies for $\Delta E_h = E_h(C_1) - E_h(C_3)$.

		Cm^{3+}		Gd^{3+}	
	symmetry	E_g [kJ mol^{-1}]	ΔE_h [kJ mol^{-1}]	E_g [kJ mol^{-1}]	ΔE_h [kJ mol^{-1}]
[M(N_4[t]bubipy)$_3$]	C_1	-5204.54	-9.6	-5280.79	-25.1
	C_3	-5193.83		-5283.06	